Range Different of Mono-Energetic 290 MeV/u Carbon Ion Across Geant4 Version with Variation of *I*-values

M. Arif Efendi[1*] & Sitti Yani[2]
[1]Department of Nuclear Engineering and Engineering Physics, Gadjah Mada University, Indonesia
[2]Department of Physics, IPB University, Indonesia
*Corresponding Author: arif.e@ugm.ac.id

Received: 28th May 2024; **Accepted**: 25th June 2024; **Published**: 29th June 2024
DOI: https://dx.doi.org/10.29303/jpft.v10i1.6933

Abstract *- The mean ionization potential (I-value) is a primary determinant of the position of the charged particle Bragg peak. To minimize their impact on beam range errors and quantify their uncertainties, the currently used I-values in Geant4 material database are revisited. The study aims at comparing set of I-values in different Geant4 versions and cross validation with PHITS Monte Carlo (MC) code. The Bragg curves of mono-energetic 290 MeV/u carbon ion beams in a Polymethyl Methacrylate (PMMA) phantom were simulated using Geant4 versions 10.6.2 and 11.2.1. Similar beam energies were replicated using the PHITS code. The Bragg curves showed good agreement between the two versions of Geant4 MC code for an I-value of 74 eV, corresponding to G4_PLEXIGLASS in the material database. When the I-value was lowered to 65 eV and 48 eV, the Bragg curves from Geant4 version 11.2.1 shifted to shallower depths. This research provides insights for evaluating the Geant4 physics model.*

Keywords*: Bragg peak; Carbon ion; Monte Carlo simulation*

INTRODUCTION

Carbon ion radiotherapy has several advantages over conventional radiotherapy with X-ray beams, primarily due to its unique Bragg peak which results in relatively low entrance doses and an optimal dose distribution (Takada, 2010). This therapy is particularly effective at targeting deeply-seated tumors that are challenging to treat because of their proximity to vital or sensitive areas of the body. Carbon ion beams enter the body with minimal radiation, travel to the tumor site, adapt to the tumor's shape and depth, and release the majority of their energy directly at the tumor location.

Charged particle therapy has seen extensive use in radiotherapy applications (Goetz and Mitic, 2018; Tsujii *et al.*, 2004). The physical and radiobiological properties of carbon ions make them particularly suitable for treating hypoxia tumors. By the end of 2023, over 57,498 patients had received treatment with carbon ions worldwide (PTCOG, 2024).

The mean ionization potential (*I*-value) of carbon ion beam is a crucial parameter in charged particle therapy, as it affects the determination of the mean excitation energy of the patient's tissues and, consequently, the dose absorbed in them. Paul (2007) compares Sihver's measured ranges of carbon ions in water, used in radiotherapy, with ranges calculated from various stopping codes and *I*-values. The best match with Sihver's experimental data is found using *I*-value of 75 eV from ICRU 49. Ranges from ICRU Report 73 and the Heinrich table are too small, while *I*-value of 80.8 eV is almost compatible within error limits. Baek *et al.* (2020) measured the stopping power of liquid water for carbon ions in the Bragg peak region using the inverted Doppler shift attenuation method. The results closely matched the data from the Errata and Addendum of ICRU Report No. 73, which uses an *I*-value of 78 eV for

water. However, the agreement was not as good when compared to the newer recommendations in ICRU Report No. 90. The SRIM code appears to slightly overestimate the stopping power of water for carbon ions above 3 MeV. Similar work has also been done with proton beams. Kumazaki *et al.* (Kumazaki *et al.*, 2007) determined the proton ranges at energies of 150, 190, and 230 MeV using Bragg curves. They found the *I*-value, which was adjusted to match the measured ranges with those predicted by the stopping power formula, to be 78.4 ± 1.0 eV. The uncertainties primarily arose from ambiguities in determining ranges from Bragg curves, errors in setting up the water phantom, and the water-equivalent thicknesses (WETs) of objects along the beam path. Bär *et al.* (2018) optimized elemental *I*-values for compounds using measured material *I*-values, considering uncertainties from experiments and their model. They assessed uncertainties on *I*-values and stopping powers for 70 human tissues, accounting for statistical correlations with water. Monte Carlo (MC) simulations evaluated how these new *I*-values impacted proton beam ranges. Their elemental *I*-values better matched measured data than ICRU recommendations (RMSE: 6.17% vs. 5.19%). They estimated a 4.42% uncertainty from a specific method. Water's *I*-value was calculated as 78.73 ± 2.89 eV, aligning with ICRU 90 (78 ± 2 eV).

The uncertainty in *I*-values is higher for inorganic materials due to their varying compositions. This study was aimed at analyzing the depth dose distributions of therapeutic energy carbon ions in Polymethyl Methacrylate (PMMA) phantom using two versions of the Geant4 MC code (Agostinelli *et al.*, 2003; Allison *et al.*, 2006, 2016) to investigate the range difference in variation of *I*-values. To validate the Geant4 simulated dose distributions, the results were compared with those obtained from PHITS MC code (Niita *et al.*, 2006; Sato *et al.*, 2024).

RESEARCH METHODS

The Bragg curves of mono-energetic 290 MeV/u carbon ion beams in a PMMA phantom were simulated using Geant4 versions 10.6.2 and 11.2.1, with cross-validation performed using PHITS code. The pencil size of the beam spot was simulated with a sigma value of 11 mm. The pencil beam spot was generated 40 cm away from the surface of the 30×30×30 cm^3 PMMA phantom. The PMMA density was set at 1.19 g/cm^3, with *I*-values of 74 eV, 65 eV, and 48 eV varied in Geant4. The pre-built QGSP_BIC_HP_EMZ Geant4 physics list was employed to model both electromagnetic and hadronic processes for both versions. These physics lists were chosen as they provided good precision in charged particle therapy, including precise neutron transport (Borja-Lloret *et al.*, 2023; Winterhalter *et al.*, 2020). The details of the prebuilt physics list are shown in Table 1. A total of 10^5 histories were simulated. The range cut was set to 1 mm, and the bin voxel size was 0.1 mm, with a step limit of 0.05 mm or half the bin size.

Table 1. Physics models used in Geant4

No	Interaction	Energy Range	Geant4 Model/Package
1	Electromagnetic	All energies	G4EmStandardPhysics_option4
2	Particle decay	All energies	G4DecayPhysics
3	Radioactive decay	All energies	G4RadioactiveDecayPhysics
4	Hadron inelastic	All energies	G4HadronPhysicsQGSP_BIC_HP

No	Interaction	Energy Range	Geant4 Model/Package
5	Hadron elastic	All energies	G4HadronElasticPhysicsHP
6	Ion Inelastic	0 – 110 MeV	Binary Light Ion Cascade
		> 100 MeV	Binary Cascade
7	Neutron Inelastic	0 – 20 MeV	NeutronHPInelastic
		> 20 MeV	Binary Cascade
8	Proton Inelastic	0 – 9.9 GeV	Binary Cascade
9	Neutron Capture	0 – 20 MeV	NeutronHPCapture

RESULTS AND DISCUSSION

Results

Figure 1 shows the Bragg curves of mono-energetic 290 MeV/u carbon ion beams simulated with Geant4 version 10.6.2 and 11.2.1 in a PMMA phantom with an *I*-value of 74 eV. The curves indicate a strong agreement between the two versions. This PMMA material replicates the G4_PLEXIGLASS material in the Geant4 Material Database, which has a density of 1.19 g/cm³ and an *I*-value of 74 eV (NIST, 2022). Figure 2 presents the Bragg curves of mono-energetic 290 MeV/u carbon ion beams simulated with Geant4 versions 10.6.2 and 11.2.1 in a PMMA phantom at an *I*-value of 65 eV. The curves begin to show disparities at this *I*-value. Figure 3 displays the Bragg curves of mono-energetic 290 MeV/u carbon ion beams simulated with Geant4 10.6.2, Geant4 11.2.1, and PHITS in a PMMA phantom at an *I*-value of 48 eV. The curves reveal that the disparity is greater compared to those with an *I*-value of 65 eV.

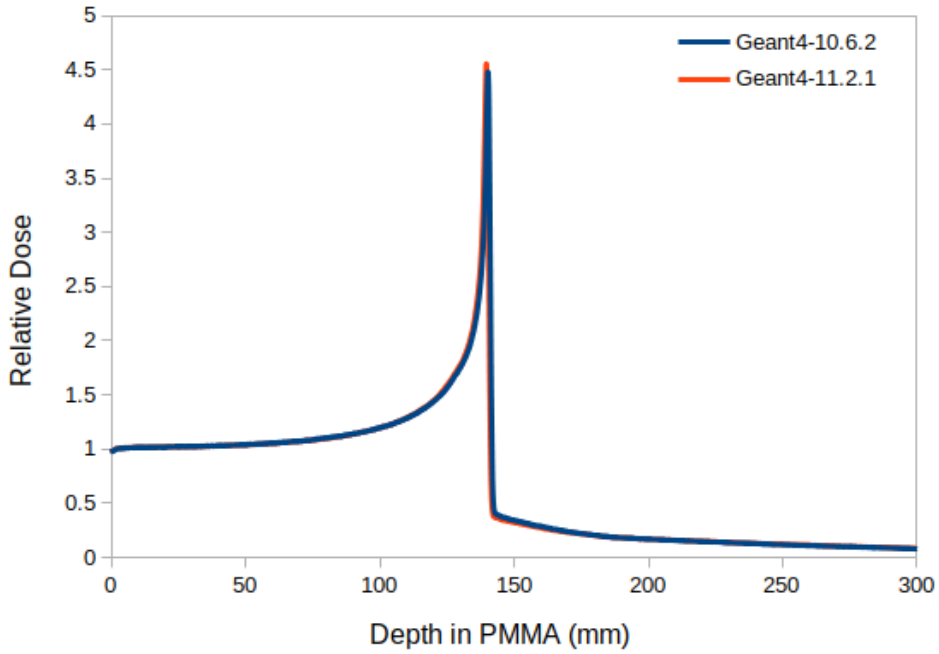

Figure 1. Comparison of Bragg curves between Geant4 10.6.2 and Geant4 11.2.1 for incident mono-energetic 290 MeV/u carbon ion beams in a PMMA phantom with an *I*-value of 74 eV

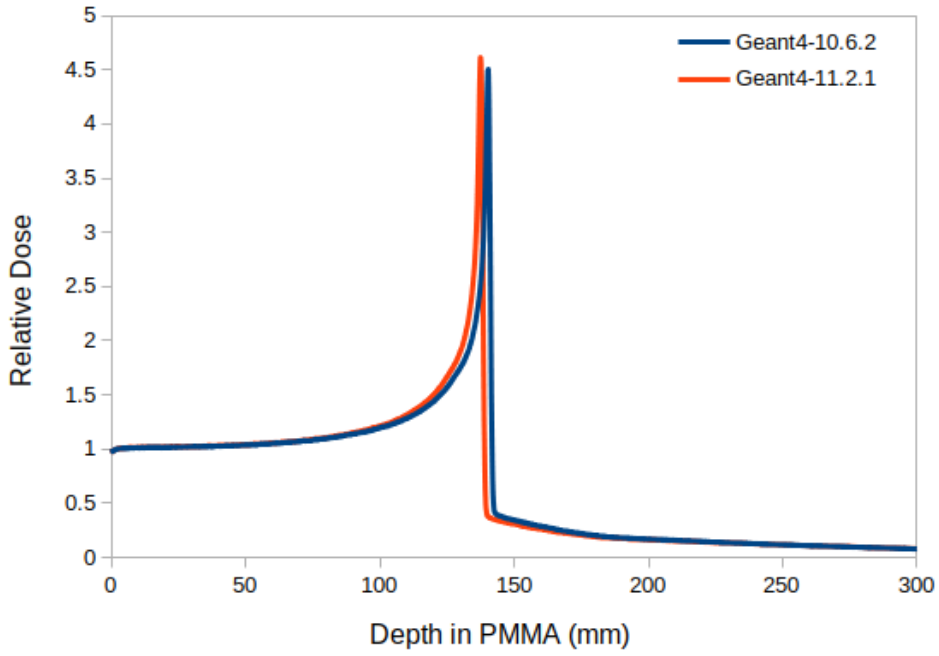

Figure 2. Comparison of Bragg curves between Geant4 10.6.2 and Geant4 11.2.1 for incident mono-energetic 290 MeV/u carbon ion beams in a PMMA phantom with an *I*-value of 65 eV

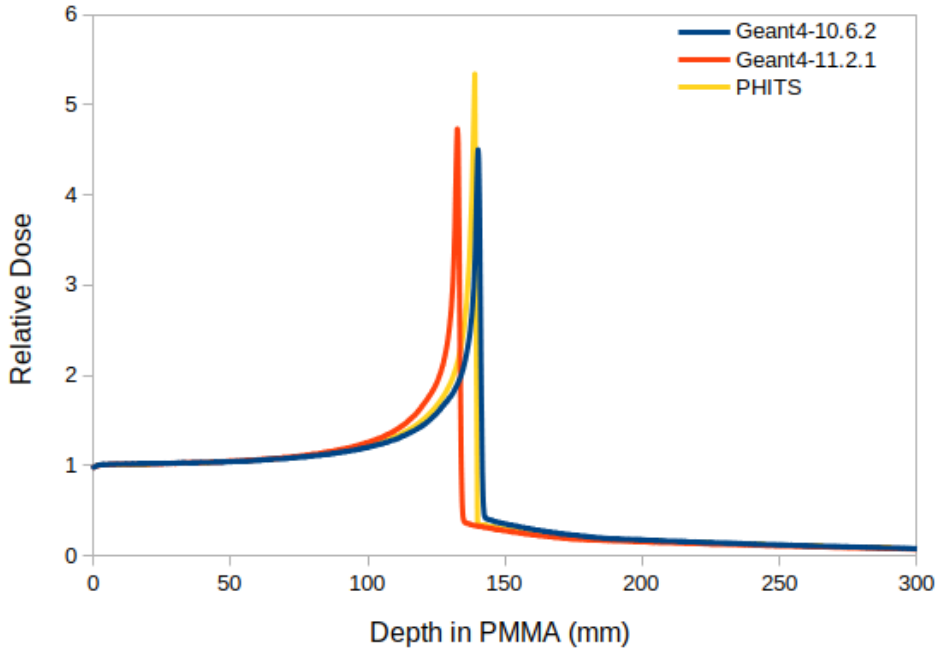

Figure 3. Comparison of Bragg curves between Geant4 10.6.2, Geant4 11.2.1, and PHITS for incident mono-energetic 290 MeV/u carbon ion beams in a PMMA phantom with an *I*-value of 48 eV

Discussion

The simulation results depict depth-dose curves for Geant4 simulation versions 10.6.2 and 11.2.1 in PMMA phantom, illustrating the characteristic Bragg peak at around 150 mm depth. Both versions show a consistent increase in dose leading up to this peak and a rapid drop-off afterward, with the peak indicating the point of maximum energy deposition by the particles. The comparison reveals that Geant4 11.2.1 has a slightly sharper and narrower Bragg peak, suggesting improvements in dose localization precision. These minor

differences highlight advancements in the newer version's physics models or computational algorithms, crucial for applications like radiation therapy where accurate dose delivery is essential. At an *I*-value of 48 eV, the difference in the Bragg curves between Geant4 10.6.2 and Geant4 11.2.1 is more pronounced. When cross-validated with PHITS, the results align with Geant4 version 10.6.2. However, the PHITS MC simulation results are sharper and show more energy deposition in the Bragg peak region, likely due to differences in energy sigma/spread. The Bragg curves also demonstrate that proportional features of dose distributions can be well described, which can be attributed in part to accurate stopping powers. This work is limited to using the pre-built QGSP_BIC_HP_EMZ Geant4 physics model to simulate an incident 290 MeV/u carbon ion on a PMMA phantom. Further simulations and validations beyond the scope of this study are required with other physics models in Geant4, such as QMD, are necessary to comprehensively investigate the range differences for various *I*-values.

CONCLUSION

A systematic investigation was conducted to evaluate the accuracy of Geant4's *I*-value for simulating Bragg curves of a carbon ion beam in a PMMA phantom. The study demonstrated that simulations using G4_PLEXIGLASS for PMMA material, based on an *I*-value of 74 eV available in the Geant4 material database, accurately reproduced the Bragg curves across Geant4 versions 10.6.2 and 11.2.1. However, the discrepancies between the two versions increased with a smaller number of *I*-values. The study indicates that further investigation into the QGSP_BIC_HP_EMZ physics model is necessary. In addition, the use of other physics models in Geant4 are also important, as well as validating the *I*-values for other materials.

ACKNOWLEDGMENT

The authors would like to thank Assoc. **Prof. Dr. Susanna Guatelli** and **Assoc. Prof. Dr. Dousatsu Sakata** for their beneficial discussions. We also extend our gratitude to the Department of Nuclear Engineering and Engineering Physics at Universitas Gadjah Mada and the Department of Physics at IPB University.

REFERENCES

Agostinelli, S., Allison, J., Amako, K., Apostolakis, J., Araujo, H., Arce, P., … Zschiesche, D. (2003). GEANT4 - A simulation toolkit. *Nuclear Instruments and Methods in Physics Research, Section A: Accelerators, Spectrometers, Detectors and Associated Equipment*, **506**(**3**), 250–303. doi:10.1016/S0168-9002(03)01368-8

Allison, J., Amako, K., Apostolakis, J., Araujo, H., Dubois, P. A., Asai, M., … Peirgentili, M. (2006). Geant4 developments and applications. *IEEE Transactions on Nuclear Science*, **53**(**1**), 270–278. doi:10.1109/TNS.2006.869826

Allison, J., Amako, K., Apostolakis, J., Arce, P., Asai, M., Aso, T., … Yoshida, H. (2016). Recent developments in GEANT4. *Nuclear Instruments and Methods in Physics Research, Section A: Accelerators, Spectrometers, Detectors and Associated Equipment*, **835**, 186–225. doi:10.1016/j.nima.2016.06.125

Baek, W. Y., Braunroth, T., De La Fuente Rosales, L., Rahm, J. M., & Rabus, H. (2020). Stopping power of water for carbon ions with energies in the Bragg peak region. *Physical Review E*, **102**(**6**), 062418. doi:10.1103/PhysRevE.102.062418

Bär, E., Andreo, P., Lalonde, A., Royle, G., & Bouchard, H. (2018). Optimized I-values for use with the Bragg additivity rule and their impact on proton stopping power and range uncertainty. *Physics in Medicine and Biology*, **63**(**16**), 165007. doi:10.1088/1361-6560/aad312

Borja-Lloret, M., Barrientos, L., Bernabéu, J., Lacasta, C., Muñoz, E., Ros, A., … Llosa, G. (2023). Influence of the background in Compton camera images for proton therapy treatment monitoring. *Physics in Medicine & Biology*, **68**(**14**), 144001. doi:10.1088/1361-6560/ACE024

Goetz, G., & Mitic, M. (2018). Carbon ion beam radiotherapy (CIRT) for cancer treatment: a systematic review of effectiveness and safety for 12 oncologic indications. *HTA-Projektbericht 101. Ludwig Boltzmann Institute for Health Technology Assessment.*, (**101**), 220. Retrieved from http://eprints.hta.lbg.ac.at/1174/%0Ahttp://eprints.hta.lbg.ac.at/1174/1/HTA-Projektbericht_Nr.101.pdf

Kumazaki, Y., Akagi, T., Yanou, T., Suga, D., Hishikawa, Y., & Teshima, T. (2007). Determination of the mean excitation energy of water from proton beam ranges. *Radiation Measurements*, **42**(**10**), 1683–1691. doi:10.1016/J.RADMEAS.2007.10.019

Niita, K., Sato, T., Iwase, H., Nose, H., Nakashima, H., & Sihver, L. (2006). PHITS-a particle and heavy ion transport code system. *Radiation Measurements*, **41**(**9**–**10**), 1080–1090. doi:10.1016/j.radmeas.2006.07.013

NIST. (2022, December). NIST Compounds: Geant4 Material Database — Book For Application Developers 10.6 documentation. Retrieved from https://geant4-userdoc.web.cern.ch/UsersGuides/ForApplicationDeveloper/html/Appendix/materialNames.html

Paul, H. (2007, February 1). The mean ionization potential of water, and its connection to the range of energetic carbon ions in water. *Nuclear Instruments and Methods in Physics Research, Section B: Beam Interactions with Materials and Atoms*. North-Holland. doi:10.1016/j.nimb.2006.12.034

PTCOG. (2024). Particle Therapy Patient Statistics (per end of 2023, provisional). Retrieved May 27, 2024, from https://www.ptcog.site/images/Statistics/Patientstatistics-provisional_Dec2023.pdf

Sato, T., Iwamoto, Y., Hashimoto, S., Ogawa, T., Furuta, T., Abe, S. I., … Niita, K. (2024). Recent improvements of the particle and heavy ion transport code system–PHITS version 3.33. *Journal of Nuclear Science and Technology*, **61**(**1**), 127–135. doi:10.1080/00223131.2023.2275736

Takada, E. (2010). Carbon Ion Radiotherapy at NIRS-HIMAC. *Nuclear Physics A*, **834**(**1**–**4**), 730c-735c. doi:10.1016/j.nuclphysa.2010.01.132

Tsujii, H., Mizoe, J. E., Kamada, T., Baba, M., Kato, S., Kato, H., … Miyamoto, T. (2004). Overview of clinical experiences on carbon ion radiotherapy at NIRS. *Radiotherapy and Oncology*, **73**(**SUPPL. 2**), S41–S49. doi:10.1016/S0167-8140(04)80012-4

Winterhalter, C., Taylor, M., Boersma, D., Elia, A., Guatelli, S., Mackay, R., … Aitkenhead, A. (2020). Evaluation of GATE-RTion (GATE/Geant4) Monte Carlo simulation settings for proton pencil beam scanning quality assurance. *Medical Physics*, **47**(**11**), 5817–5828. doi:10.1002/mp.14481